

Multimodal imaging of striatal degeneration in Amish patients with glutaryl-CoA dehydrogenase deficiency

Kevin A. Strauss,¹ Jelena Lazovic,² Max Wintermark³ and D. Holmes Morton¹

¹Clinic for Special Children, Strasburg, PA, ²California Institute of Technology, Department of Biology, Pasadena, CA and

³University of California, San Francisco, Department of Radiology, Neuroradiology Section, San Francisco, CA, USA

Correspondence to: Kevin A. Strauss, MD, Clinic for Special Children, 535 Bunker Hill Road, Strasburg, PA 17579, USA

E-mail: kstrauss@clinicforspecialchildren.org

Despite early diagnosis, one-third of Amish infants with glutaryl-CoA dehydrogenase deficiency (GAI) develop striatal lesions that leave them permanently disabled. To better understand mechanisms of striatal degeneration, we retrospectively studied imaging results from 25 Amish GAI patients homozygous for 1296C>T mutations in GCDH. Asymptomatic infants had reduced glucose tracer uptake and increased blood volume throughout gray matter, which may signify a predisposition to brain injury. Nine children (36%) developed striatal lesions: three had sudden motor regression during infancy whereas six had insidious motor delay associated with striatal lesions of undetermined onset. Acute striatal necrosis consisted of three stages: (1) an acute stage, within 24 h of motor regression, characterized by cytotoxic oedema within the basal ganglia, cerebral oligemia, and rapid transit of blood throughout gray matter; (2) a sub-acute stage, 4–5 days after the onset of clinical signs, characterized by reduced striatal perfusion and glucose uptake, and super-vening vasogenic oedema; and (3) a chronic stage of striatal atrophy. Apparent diffusion coefficient maps revealed that at least two of the six patients with insidious motor delay suffered striatal injuries before or shortly after birth, followed by latent periods of several months before disability was apparent. Thus, acute and insidious presentations may occur by similar mechanisms, and differ only with regard to the timing of injury. Intravenous fluid and dextrose therapy for illnesses during the first 2 years of life was the only intervention that was clearly neuroprotective in this cohort (odds ratio for brain injury = 0.04, 95% confidence interval = 0.01–0.34; $P < 0.001$).

Keywords: glutaric aciduria type I; striatal necrosis; diffusion; perfusion; cerebral metabolism

Abbreviations: ADC = apparent diffusion coefficient; CBF = cerebral blood flow; CBV = cerebral blood volume; CI = confidence interval; CSF = cerebrospinal fluid; FDG = 2-[¹⁸F]fluoro-2-deoxy-D-glucose; GAI = glutaric aciduria type I; GCDH = glutaryl-CoA dehydrogenase; LDH = lactate dehydrogenase; MRI = magnetic resonance imaging; MTT = mean transit time; OR = odds ratio; PCT = perfusion computed tomography; PET = positron emission tomography; SUV_{bsa} = standard uptake value corrected for body surface area.

Received September 17, 2006. Revised February 12, 2007. Accepted March 2, 2007. Advance Access publication May 3, 2007

Introduction

Glutaryl-CoA dehydrogenase deficiency (GCDH; glutaric acidemia type 1, GAI) is a disorder of lysine and tryptophan degradation that results in accumulation of glutaric and 3-hydroxyglutaric acid in the brain and other tissues (Kolker *et al.*, 2003; Funk *et al.*, 2005). The incidence of GAI is high among the Old Order Amish of Pennsylvania, where approximately 1 in 500 children are born homozygous for missense mutations in the *GCDH* gene (1296C>T, A421V). Between 1989 and 2005, we have provided medical care for 48 such children (Morton *et al.*, 1991; Strauss *et al.*, 2003).

Striatal degeneration is the most serious consequence of GAI, and often leaves children neurologically devastated (Strauss *et al.*, 2003). In our practice, we recognize two patterns of motor disability. After a period of normal development, some infants suddenly regress during an infectious illness or surgery, and on magnetic resonance imaging (MRI) have evidence of acute cytotoxic oedema within the basal ganglia. A second group of children have motor delays from early infancy, and on MRI have atrophic striatal lesions of undetermined onset.

Whether acute or insidious in onset, striatal degeneration remains an unpredictable and poorly understood event.

Specifically, it is not clear whether injury to neurons is caused by direct actions of a histotoxin, ischaemia or both. Uncertainty about the mechanisms of brain injury is reflected in use of the term *metabolic stroke* (Hoffmann *et al.*, 1994; Haas *et al.*, 1995), which lacks a precise definition (Auer and Sutherland, 2002). *In vitro* studies cannot clarify the issue because they do not model interactions between metabolism and blood flow characteristic of the living brain (Clarke and Sokoloff, 1999).

To investigate this problem, we conducted a retrospective study focused on two aims: (1) to more precisely define the relative importance of metabolic and hemodynamic alterations in the pathophysiology of striatal degeneration, and (2) to explore what specific treatments, if any, reduce the risk for this injury. To address the first aim, we studied imaging data from the 25 youngest Amish patients under our care, born between 1995 and 2005. We chose to concentrate on this group because they were treated in a relatively consistent fashion and could be studied with modern quantitative imaging techniques. In order to better understand the sequence of histological events, we were careful to match imaging results to clinical context.

To address the second aim, we reviewed the records of all 48 Amish GA1 patients cared for at our clinic since its inception in 1989. Among this larger group, a total of 28 subjects were disabled and had striatal lesions on MRI. We investigated how specific interventions (e.g. diet strategy, L-carnitine therapy, etc.) affected the risk for brain injury. Restricting the focus to local Amish patients limited confounding factors in this analysis: all of the

patients were cared for at a single clinical centre by two of the authors (DHM and KAS), quantitative treatment variables were accurately known, affected children were all homozygous for the same *GCDH* mutation, and environmental and genetic background variations were minimized (Morton *et al.*, 2003; Puffenberger, 2003).

Patients and Methods

Patients

The study was approved by the Institutional Review Board of Lancaster General Hospital. Written informed consent was obtained for molecular testing.

A total of 48 Amish individuals homozygous for *GCDH* 1262C>T were managed at our clinic since 1989. We divided them into four groups based on birth year to reflect major shifts in the timing of diagnosis and the specifics of therapy (Table 1). Seventeen patients were identified before the advent of newborn screening (pre-1990 group); all of them but one were crippled by striatal lesions. (Between 1989 and 1994, population-based testing for GA1 was done on 1212 Amish individuals to minimize the possibility that asymptomatic untreated GA1 patients were not ascertained. Only one asymptomatic GA1 patient was found.) All 31 children born after 1989 were diagnosed as asymptomatic newborns. For the present study, we focused on the 25 youngest children within this latter group, born between 1995 and 2005, which included 10 male and 15 female children (mean age 67 months; age range 16–146 months).

We chose to concentrate on the 25 youngest children for three reasons: (1) they were treated in similar fashion with regard to L-carnitine dose, dietary lysine and tryptophan intake, and emergency care during illnesses (Tables 1 and 2) (see online

Table 1 Incidence of brain injury based on birth year and outpatient treatment strategy for 48 Amish GA1 patients

| | Birth year | | | |
|--|------------|-----------|-----------|-----------|
| | Pre-1990 | 1990–1994 | 1995–2002 | 2003–2005 |
| Group characteristics | | | | |
| Total number of patients (n) | 17 | 6 | 14 | 11 |
| Diagnosed by newborn screening (%) | 0 | 100 | 100 | 100 |
| Treatment variables | | | | |
| Emergency inpatient management during illnesses (%) | 0 | 100 | 100 | 100 |
| Diet low in natural protein, 1.0–1.3 g/kg/day (%) | 0 | 100 | 100 | 100 |
| L-carnitine therapy, 75–100 mg/kg/day (%) | 0 | 0 | 100 | 100 |
| Lysine-free amino acid supplement, 0.5–1.0 g/kg/day (%) ^a | 0 | 0 | 7 | 82 |
| Vitamin cofactor supplement, 80–120 mg/kg/day (%) | 0 | 0 | 14 | 73 |
| Prophylactic anticonvulsant therapy, 0–12 months (%) ^b | 0 | 0 | 64 | 45 |
| Outcomes | | | | |
| Brain injury (%) | 94 | 50 | 36 | 36 |
| • Acute motor regression (n) | na | 2 | 2 | 1 |
| • Insidious motor delay (n) | na | 1 | 3 | 3 |
| Untimely death (n) | 7 | 2 | 0 | 0 |

^aIn 2002, we began supplementing the diet with lysine-free L-amino acids. Injury rate did not differ based on dietary strategy: injury rate with low-protein diet + lysine-free L-amino acids was 30% (n = 10); injury rate with low-protein diet only was 40% (n = 15) (Fisher's exact test, *P* = 0.690).

^bMost patients born between 1995 and 2002 received a prophylactic anticonvulsant from birth to 12 months. Anticonvulsants were not given prophylactically to patients born after 2004. Injury rate did not differ based on anticonvulsant treatment: injury rate with anticonvulsant therapy was 38% (n = 13); injury rate with no anticonvulsant therapy was 33% (n = 12) (Fisher's exact test, *P* = 1.000). na = data not available.

Supplementary material); (2) they could be divided into two distinct subgroups with regard to lysine-free supplemental L-amino acid therapy (see online Supplementary material); and (3) digital imaging files could be used to quantitate water diffusion, fluorodeoxyglucose uptake and blood flow for regions of interest depicted in Fig. 1.

Patients born between 1995 and 2005 were further divided into brain-injured and asymptomatic groups. Inclusion in the brain-injured group required the presence of both extrapyramidal clinical signs and striatal lesions visible with MRI. In our experience, motor disability and striatal lesions always co-exist in patients with GAI (Strauss *et al.*, 2003). Brain images were designated *acute* if obtained within 24 h of sudden motor regression. A *sub-acute* stage was also identified, based on a characteristic pattern of diffusion changes occurring 4 to 5 days after lesion onset (Lansberg *et al.*, 2001; Walker *et al.*, 2004).

Images obtained greater than 2 months after the first radiographic signs of injury consistently showed focal atrophy in the striatum, and were designated the *chronic* stage. Subjects with GAI that did not develop striatal lesions were labelled *asymptomatic*. Imaging data from one additional non-Amish GAI patient were included, with parental consent, to construct Fig. 2.

For MRI diffusion studies, control data consisted of 20 measurements (right and left hemisphere) for each region of interest, taken from 10 control subjects (ages 24 ± 19 months, age range 0.5–61 months). These children were under our care for other medical conditions and had normal results of brain imaging undertaken for standard indications, such as meningitis, head trauma, seizure, ataxia and developmental delay. For perfusion computed tomography (PCT) studies, control data were taken from two children (four measurements for each region of interest) ages 7 months (meningitis) and 79 months (ataxia). For both

Table 2 Amish GAI cohort (GCDH I296C>T/I296C>T) born between 1995 and 2005 (N = 25)

| | Amish children with GAI (GCDH I296C>T) | | |
|---|--|-----------------------|------------------|
| | Injured (N = 9) | Asymptomatic (N = 16) | Reference values |
| Growth and development | | | |
| Weight gain, birth to 6 months (g/day) | 23.5 ± 3.9 | 24.7 ± 4.5 | 18.3–28.9 |
| Head growth, birth to 6 months (OFC in mm/day) | 0.48 ± 0.15 | 0.48 ± 0.08 | 0.38–0.62 |
| Head circumference relative to BSA, 0–6 months (cm/m^2) | 137.4 ± 17.3 | 140.0 ± 23.1 | 102–132 |
| Age at independent sitting (months) | 12.2 ± 2.8 | 6.9 ± 1.0^a | 5.5–70 |
| Age at independent standing (months) | NA ^b | 12.5 ± 1.1 | 10.5–13.5 |
| Clinical encounters | | | |
| Office visits per month, birth to 12 months | 0.7 ± 0.4 | 0.8 ± 0.3 | NA |
| Hospitalizations for illness, 0–18 months | 2.1 ± 1.5 | 2.4 ± 1.7 | NA |
| Maintenance Diet | | | |
| Total protein intake (g/kg/day) ^c | 1.3 ± 0.3 | 1.4 ± 0.3 | 1.4–2.3 |
| Lysine intake (mg/kg/day) | 75 ± 17 | 79 ± 16 | 98–177 |
| Percentage total protein as lysine (%) | 6.0 ± 1.5 | 6.1 ± 1.6 | 6.0–8.0 |
| Tryptophan intake (mg/kg/day) | 22 ± 6 | 24 ± 7 | 24–39 |
| Calorie intake (kcal/kg/day) | 100 ± 15 | 95 ± 9 | 85–115 |
| L-carnitine dose (mg/kg/day) | 80 ± 36 | 79 ± 27 | NA |
| Routine Outpatient Biochemical Monitoring | | | |
| Plasma lysine ($\mu\text{mol}/\text{l}$) ^d | 90 ± 30 | 116 ± 50 | 135 \pm 55 |
| Plasma tryptophan ($\mu\text{mol}/\text{l}$) | 21 ± 18 | 27 ± 14 | 42 \pm 10 |
| Plasma glutarate ($\mu\text{mol}/\text{l}$) ^e | 6.18 ± 1.30 | 4.89 ± 1.80 | ND |
| Plasma 3-hydroxyglutarate ($\mu\text{mol}/\text{l}$) | 1.45 ± 0.38 | 1.23 ± 0.70 | ND |
| Plasma glutarate/3-hydroxyglutarate ratio (mol : mol) | 4.81 ± 1.93 | 4.85 ± 1.33 | NA |
| Serum glutaryl carnitine ($\mu\text{mol}/\text{l}$) | 0.67 ± 0.25 | 0.64 ± 0.45 | <0.09 |
| Serum total carnitine ($\mu\text{mol}/\text{l}$) | 72 ± 24 | 72 ± 29 | 17–41 |
| Serum free carnitine ($\mu\text{mol}/\text{l}$) | 47 ± 16 | 49 ± 27 | 10–21 |
| Urine glutarate ($\mu\text{mol}/\text{mmol Cr}$) ^f | 67 ± 45 | 90 ± 53 | <15 |
| Urine 3-hydroxyglutarate ($\mu\text{mol}/\text{mmol Cr}$) | 145 ± 59 | 120 ± 40 | <4 |
| Urine glutaryl carnitine ($\mu\text{mol}/\text{mmol Cr}$) | 19 ± 15 | 18 ± 14 | <5.2 |

^aStudent's *t*-test, *P* = 0.006.

^bAmong 9 brain-injured patients, 3 never sat alone and 7 never stood alone; 2 injured patients stood alone at 24 and 42 months.

^cTotal protein intake was the sum of protein from natural sources (1.15 ± 0.15 g/kg/day) and, for 10 children, 0.5–1.0 g/kg/day of a lysine-free L-amino acid mixture (for composition, see Table 5). Values for total protein intake for each group are lower than might be expected, because only 33% of injured and 44% of non-injured patients were taking a lysine-free L-amino acid supplement. The range of total protein intakes for patients taking supplemental lysine-free amino acids was 1.5–2.1 g/kg/day.

^dCord blood lysine values were 320–330 $\mu\text{mol}/\text{l}$ and decreased into the normal range over the first 24–48 h of life.

^eOrganic acids were higher in cord blood (glutarate 70–113 $\mu\text{mol}/\text{l}$, 3-hydroxyglutarate 4–6 $\mu\text{mol}/\text{l}$) and amniotic fluid (glutarate 90–120 $\mu\text{mol}/\text{l}$).

^fUrine glutarate and 3-hydroxyglutarate values (mean \pm SD) are for specimens obtained from children ≥ 1 month of age during routine outpatient monitoring. Total urine glutarates were much higher (up to 5500 $\mu\text{mol}/\text{mmol Cr}$) during the perinatal transition, and could increase considerably during illnesses. Values for urine 3-hydroxyglutarate are higher than previously reported (Strauss *et al.*, 2003) due to improved quantitation using a deuterated internal standard.

NA = not applicable; ND = not detected.

practical and ethical reasons, only adult control data ($n=3$, ages 20–21 years) were available to compare to positron emission tomography (PET) results from five children with GA1 (ages 6, 9 and 12 months, and 10 and 12 years).

Magnetic resonance imaging and apparent diffusion coefficient mapping

Magnetic resonance imaging was performed on a 1.5 T Siemens Symphony system (Siemens Medical Systems). Tissue dimensions and venous diameters were measured with DicomWorks region of interest software (<http://dicom.online.fr/>). We chose to measure diameter of the vein of Galen for three reasons: (1) it can be reliably identified on coronal T2-weighted MRI, (2) it drains the majority of striatal blood flow and (3) unlike the dural venous sinuses, it is compliant (i.e. distensible), and therefore might reflect volume changes within the deep cerebral venous system.

For apparent diffusion coefficient (ADC) mapping, 20 axial diffusion-weighted slices were acquired using a single shot echo planar sequence (TE/TR = 125/4600 ms, 5 mm slice thickness, 1.5 mm slice separation, FOV = $20 \times 20 \text{ cm}^2$, 128×128 matrix size and 1 average). A T2-weighted image ($b=0 \text{ s/mm}^2$) and two diffusion-weighted images ($b=500$ and 1000 s/mm^2) with three orthogonal gradients were obtained for each slice. Resulting diffusion trace images were generated for each of the three b -values. An ADC was calculated pixel by pixel as the negative slope of a line fitting the three points for b versus the natural logarithm of signal intensity. Image analysis was accomplished using CCHIPS/IDL software (Schmithorst *et al.*, 2001) and ADC values were recorded for regions of interest depicted in Fig. 1 and reported in units $\times 10^{-3} \text{ mm}^2/\text{s}$.

Fluorodeoxyglucose positron emission tomography

2- ^{18}F fluoro-2-deoxy-D-glucose (FDG, 0.15 mCi/kg, minimum dose 2.5 mCi, maximum dose 10 mCi) was administered over

30 s via peripheral vein and allowed to circulate for 45–60 min prior to image acquisition on a Siemens ECAT ACCEL 3D scanner equipped with a lutetium oxyorthosilicate detector. Attenuated standard uptake values were normalized to body surface area (SUV_{bsa}) according to standard formulae (Sugawara *et al.*, 1999; Yeung *et al.*, 2002):

$$\text{SUV}_{\text{bsa}} = \frac{C_{\text{roi}}}{D_t/\text{BSA}}$$

$$\text{BSA in } m^2 = 0.007184 (\text{weight in kg})^{0.425} (\text{length in cm})^{0.725}$$

where C_{roi} is tissue tracer concentration in Bq/ml corrected to acquisition start time and D_t is the time-corrected tracer dose in Bq. Three of the eight patients studied with PET received lorazepam (0.1 mg/kg) prior to imaging. For these subjects, 'corrected' SUV_{bsa} values were estimated to be 13% higher than measured values to account for the depression of cerebral glucose consumption caused by benzodiazepines (Wang *et al.*, 1996).

Although we minimized systematic errors by correcting standard uptake values for body surface area, tracer decay and drug effects, we still had to rely on adult control data for comparisons. We recognize this as a problem; FDG uptake by the adult brain is 10–15% higher than that of 6- to 12-month old infants (Nehlig, 1997; Erecinska *et al.*, 2004). However, this difference does not change the main conclusions of Fig. 3, and does not account for the *regionally selective* pattern of glucose hypometabolism we found in GA1 infants.

Perfusion computed tomography

Perfusion data were obtained using a standard pediatric protocol (Wintermark *et al.*, 2001, 2004). Briefly, an age- and weight-based dose of low-osmolarity non-ionic iodinated contrast was administered by peripheral vein with a power injector. Two 10 mm thick slices containing the basal ganglia, and selected above the orbits to protect the lenses, were assessed. Perfusion CT data consisted of

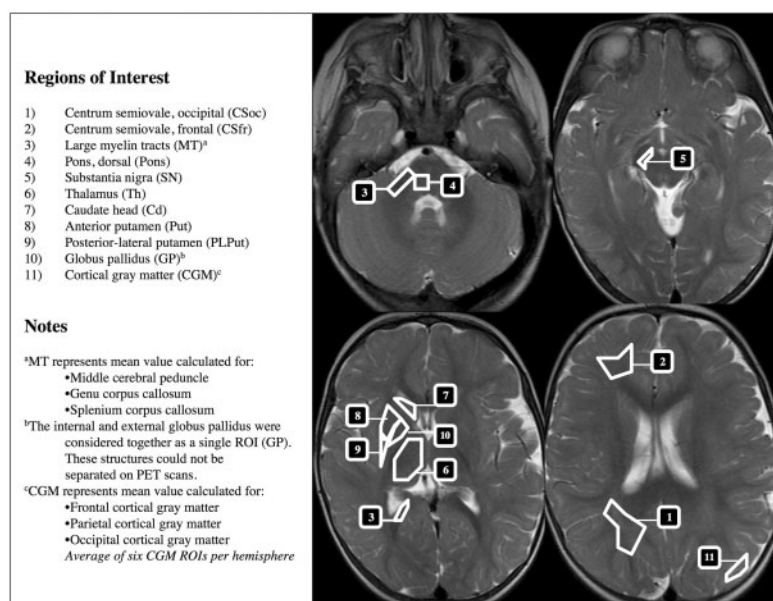


Fig. 1 Region of interest scheme. Modifications were used for ADC, FDG PET and perfusion CT studies.

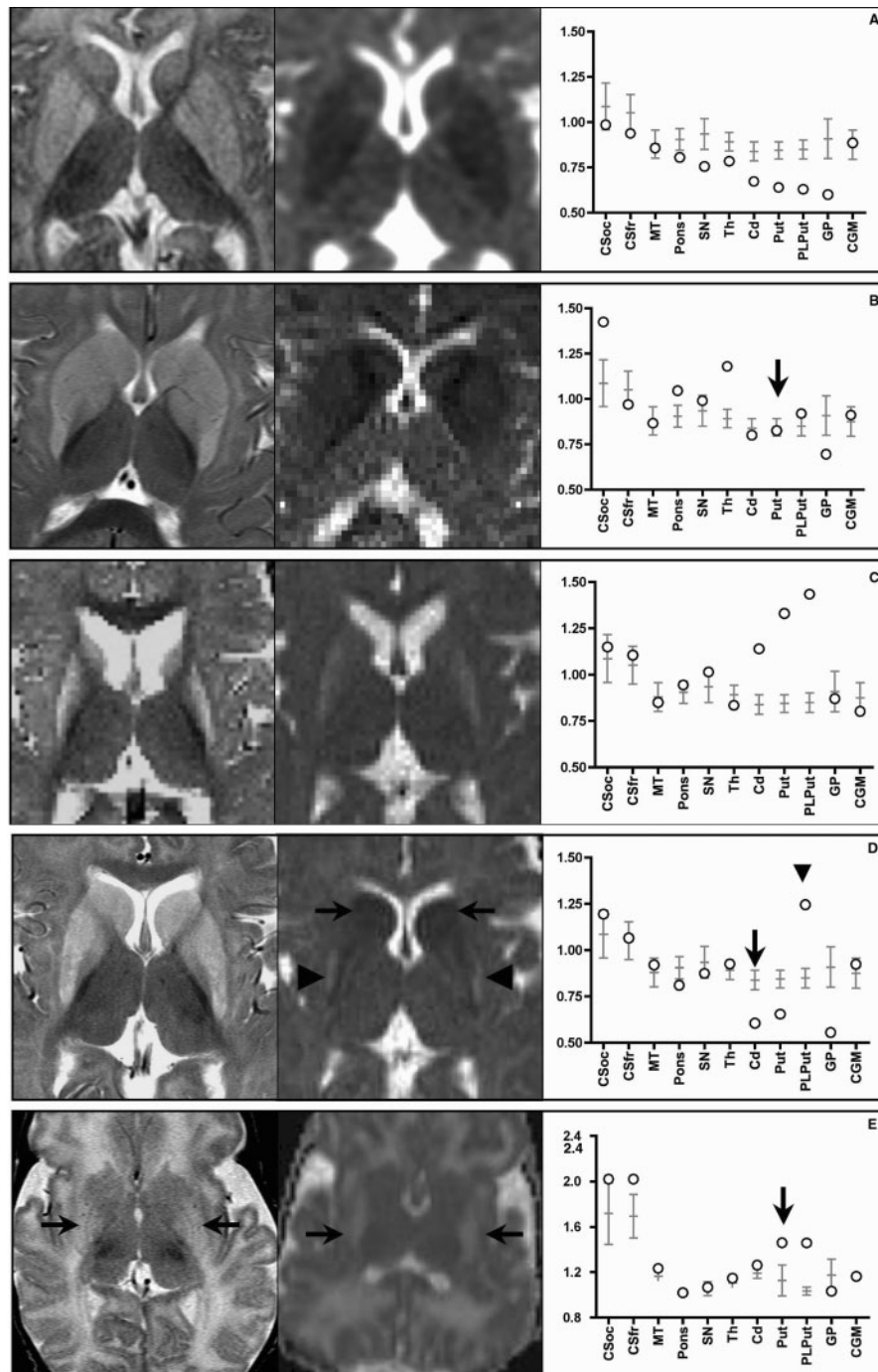


Fig. 2 Apparent diffusion coefficient maps of children with GAI. Each panel displays, left to right, a T2 axial of the basal ganglia, a corresponding ADC map and a plot of quantitative ADC values ($\times 10^{-3} \text{ mm}^2/\text{s}$) for each region of interest (white circles). Control data consist of 20 measurements from 10 children (mean age 24 months, age range 0.5–61 months), and are shown as gray mean \pm 2 standard deviation bars. **(A)** *Acute cytotoxic stage*: a 24–34% reduction in diffusion is seen throughout the basal ganglia, which are not swollen. **(B)** *Sub-acute vasogenic stage*: physical swelling and 'normalization' of ADC values in the caudate and putamen (arrow) represents a composite of cytotoxic (intracellular) and supervening vasogenic (extracellular) edema (Case 1). Pallidal (i.e. GP) ADC values remain low. **(C)** *Chronic atrophic stage*: three months following acute regression, striatal neurons have died in a posterior-to-anterior gradient, resulting in reduced tissue volume and high diffusion associated with focal gliosis. Pallidal ADC values have returned to normal, suggesting recovery. **(D)** An 8-month-old child (Case 2) was imaged in the setting of acute motor regression. He had characteristic cytotoxic ADC changes of the anterior striatum (arrows) superimposed on old atrophic lesions of the posterior-lateral putamen (arrowheads). **(E)** Two neonates with GAI were imaged at 2 weeks of age (Case 3), at which time they were asymptomatic. Both children had high-diffusion striatal lesions (arrows), and subsequently developed motor delay and dystonia during infancy (control data depicted in panel E represent eight measurements, right and left, taken from four neonates: two without GAI as well as two with GAI that did not develop brain injury). *Abbreviations*: see Fig. 1.

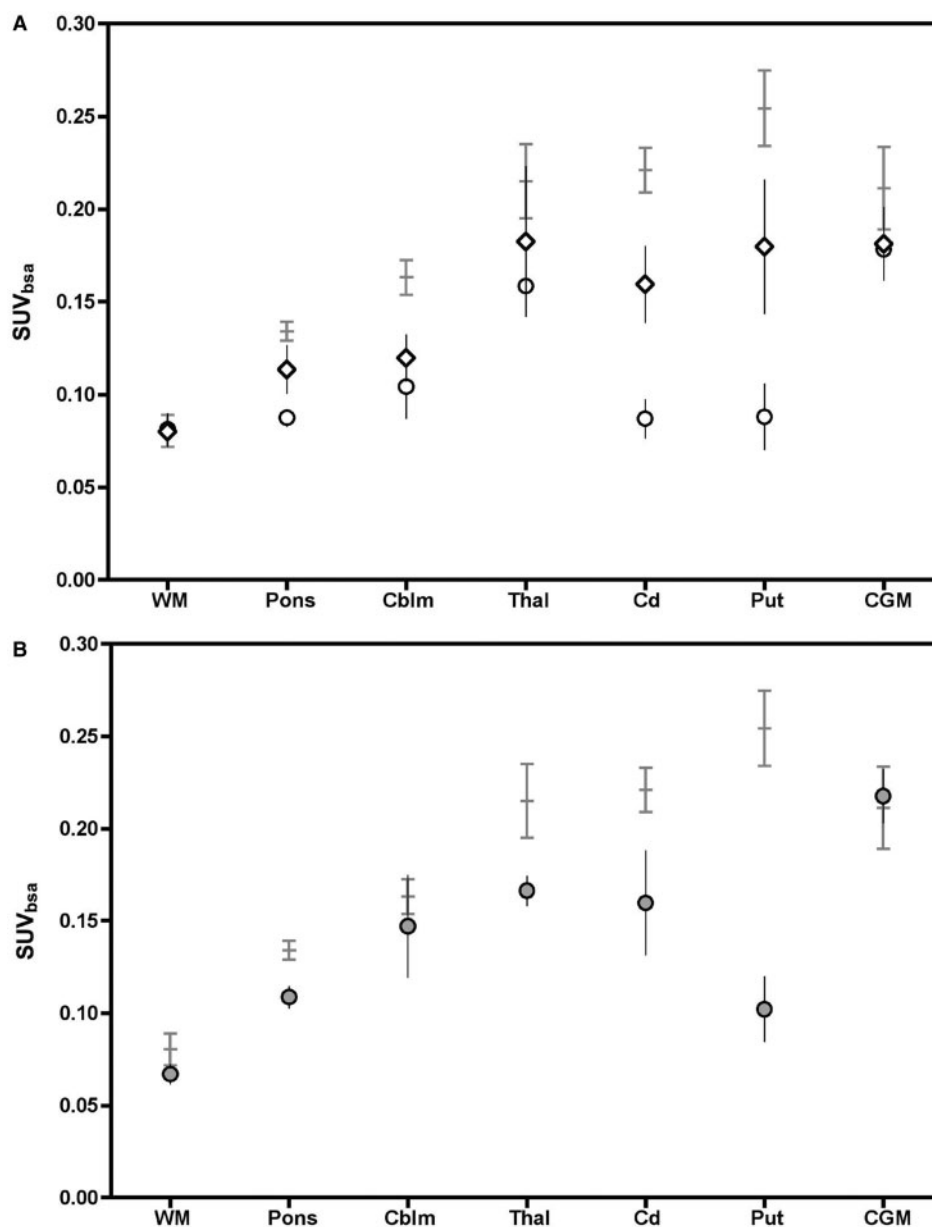


Fig. 3 Regional cerebral FDG uptake (mean \pm SD). **(A)** Two asymptomatic infants (white diamonds) and a 12-month-old child during the sub-acute stage of acute striatal necrosis (Case 1; white circles) had selectively reduced striatal and cerebellar FDG uptake relative to healthy adults ($n = 3$, ages 20–21 years; gray bars). **(B)** In two GAI patients with static atrophic striatal lesions (e.g. Case 4, gray circles), there was a gradient of impaired striatal FDG uptake. PET data is presented conservatively; differences were larger when SUV values were corrected for lean body mass (data not shown), and correction for benzodiazepine effects (Wang *et al.*, 1996) narrowed the differences between study groups. Abbreviations: see Fig. 2.

time-contrast enhancement curves registered in each pixel and linearly related to time-concentration curves for the iodinated contrast material. Data were filtered spatially and temporally and analysed with PCT software as previously described (Wintermark *et al.*, 2004). Cerebral blood volume (CBV; ml/100 g) was divided by mean capillary blood transit time (MTT; seconds) to calculate cerebral blood flow (CBF, in ml/100 g per minute) for selected regions of interest (Fig. 1).

Data analyses

Table 3 lists the number of subjects in each study group. For MRI, ADC, PET and PCT studies, measurements from each hemisphere

were considered independently, and vein of Galen diameter was measured along two perpendicular axes for each patient. Thus, the number of independent data points for imaging studies was twice the number of subjects. Data were depicted as means \pm standard deviations, except where indicated otherwise. Statistical calculations were performed using Prism 4 software (GraphPad Software, San Diego, CA, USA). Clinical and biochemical characteristics of brain-injured and asymptomatic subjects were compared using the two-tailed Student's *t*-test (Table 2). Imaging data sets that included three or more experimental groups (e.g. control, asymptomatic, acute, chronic) were analysed with one-way analysis of variance (ANOVA) followed by the Tukey post-test

Table 3 Number of subjects^a for each study condition

| | Control | Amish children with GAI (GCDH I296C>T) | | | | |
|------------------------|-----------------|--|-------------|-------------------|-----------------------|--------------------|
| | | Newborn | Not injured | Acute (Cytotoxic) | Sub-acute (Vasogenic) | Chronic (Atrophic) |
| Diffusion (ADC) map | 10 ^b | 4 | 1 | 1 | 1 | 9 |
| Vein of Galen diameter | 8 | — | — | 1 | 2 | 9 |
| Fluorodeoxyglucose PET | 3 ^c | — | 2 | — | 1 | 2 |
| Perfusion CT | 2 ^d | — | 2 | 1 ^e | 1 ^e | 2 |

^aFor each subject, each region of interest was measured on the right and left side of the brain; both values were used for statistical calculations.
^bControl subjects were 24 ± 19 months of age (age range 0.5–61 months). Two newborns (age 2–3 weeks) without GAI served as controls for four GAI newborns.
^cThree control subjects used for PET studies were 20–21 years old.
^dPerfusion CT control subjects were ages 7 months (meningitis) and 79 months (ataxia).
^eThe same individual (age 8 months) was scanned during the acute cytotoxic (10 h) and subacute vasogenic (100 h) stages of striatal injury.

to compare differences between groups (Table 4). Tukey *P*-value approximations <0.05 were accepted as significant. Differences in treatment were analysed as paired contingencies (timing of diagnosis, year of birth, dietary strategy, L-carnitine supplementation, vitamin cofactor therapy, prophylactic anticonvulsant therapy, perinatal hospitalization and immunization) and studied with a two-sided Fisher's exact test. Results were reported as an odds ratio (OR) and 95% confidence interval (CI) for brain injury relative to the intervention of interest.

Results
Case summaries

Four cases are briefly summarized to illustrate the various clinical circumstances under which images were obtained. A more detailed summary of imaging results follows.

Case 1: acute striatal necrosis during an infectious illness

An Amish girl born at term was diagnosed with GAI as a newborn by analysis of organic acids in cord blood and amniotic fluid. She was admitted to the hospital at 5 days of age and started on a low-protein diet (lysine intake 75 ± 11 mg/kg/day, tryptophan intake 17 ± 3 mg/kg/day), L-carnitine (85 mg/kg/day) and diazepam (0.6–1.0 mg/kg/day). Growth was normal along the 90th percentile for weight and 95th percentile for head circumference. She sat independently at 6.5 months and cruised at 11 months. Shortly after her first birthday, she developed simultaneous bronchiolitis and *Escherichia coli* urinary tract infection, and was sick at home for 3 days before she suddenly regressed. At the hospital 8 h later, her temperature was 39.4°C. She was tachypneic, dehydrated and flaccid. A brain MRI 48 h after admission showed focal swelling, venous congestion and 'pseudo-normal' ADC values (0.79–0.95 × 10^{−3} mm²/s; normal 0.85 ± 0.05 × 10^{−3} mm²/s) (Nagesh *et al.*, 1998; Walker *et al.*, 2004) throughout the striatum (Fig. 2B). The vein of Galen was markedly dilated

(diameter 0.72 cm; normal 0.38 ± 0.10 cm) (Fig. 4). Striatal FDG uptake was reduced to ~35% of control values (Fig. 3A, white circles). Striatal tissue atrophied over ensuing months (Fig. 2C). The child is now 6 years old and fully disabled; she is mute, fed through a gastrostomy tube, confined to a wheelchair and unable to use her hands.

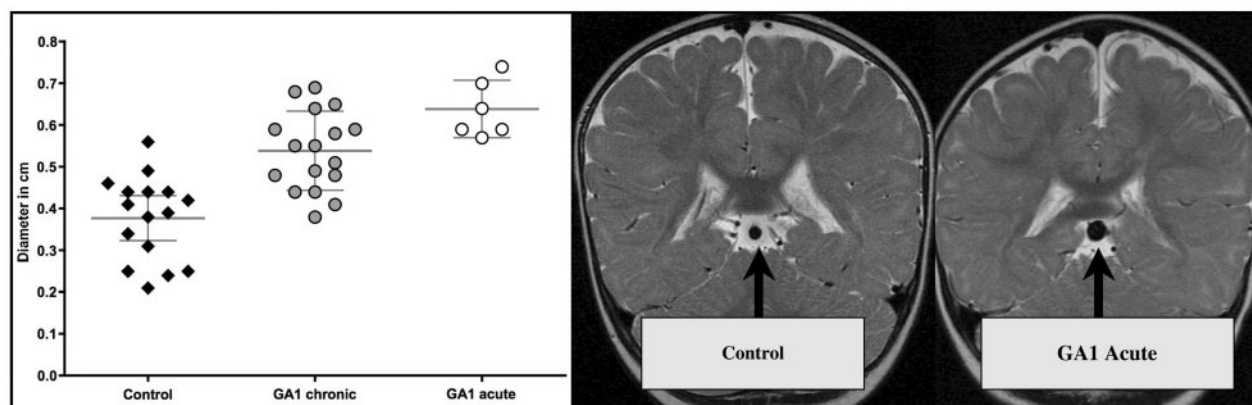
Case 2: acute striatal necrosis with no precipitant, superimposed on existing lesions

An Amish boy was diagnosed with GAI on day 1 of life by metabolite analysis of cord blood (glutarate 13 µmol/l, 3-hydroxyglutarate 2.3 µmol/l, glutarylcarntine 0.35 µmol/l) and amniotic fluid (glutarate 113 µmol/l, 3-hydroxyglutarate 17 µmol/l, glutarylcarntine 4.9 µmol/l). He was treated with a low-protein diet (lysine intake 71 ± 9 mg/kg/day, tryptophan intake 24 ± 4 mg/kg/day), lysine-free L-amino acids (0.5 g/kg/day) and L-carnitine (80 mg/kg/day), but was not treated with an anticonvulsant. He was seen in the office monthly and received all immunizations. Weight and length increased normally along the 50th percentile, head growth was stable along the 95th percentile, and general health was excellent. At his 6-month office visit, he had mild hypotonia of the trunk and chorea of the distal upper limbs. At age 7 months, he could not sit independently, but he could control his head and use his hands. At age 8 months, he unexpectedly developed acute opisthotonus. He was admitted to hospital, where his vital signs, general physical examination and routine laboratory studies were normal.

A PCT scan done 10 h after he developed opisthotonus showed normal density of the striatum, global reductions of cerebral blood volume and transit time, hyperperfusion of the caudate (112.9 ml/100 g/min; control values for striatum 72.2 ± 4.2 ml/100 g/min) and normal blood flow to the putamen (67.7 ml/100 g/min) (Fig. 5). A PCT scan 90 h later showed lucency of the striatum and reduced perfusion

Table 4 Summary statistics for diffusion, glucose tracer uptake, and perfusion data

| Region of interest | Control | Amish children with GAI (GCDH I296C>T) | | | |
|--|--------------|--|--------------------------------|------------------------------------|----------------------------|
| | | Asymptomatic | Acute (Cytotoxic) ^a | Sub-acute (Vasogenic) ^a | Chronic (Atrophic) |
| Putamen | | | | | |
| ADC (×10 ⁻³ mm ² /s) | 0.85 ± 0.05 | 0.84 | 0.64 ^{b,c} | 0.83 | 1.22 ± 0.22 ^{d,e} |
| FDG SUV _{bsa} | 0.25 ± 0.02 | 0.18 ± 0.04 ^b | — | 0.09 ^{b,c} | 0.10 ± 0.02 ^{b,c} |
| CBF (ml/100 g/min) | 75.76 ± 5.44 | 89.32 ± 20.05 | 67.70 | 39.96 ^b | 68.30 ± 21.48 |
| CBV (ml/100 g) | 5.59 ± 0.75 | 6.75 ± 0.55 ^d | 3.44 ^{b,c} | 3.32 ^{b,c} | 5.42 ± 1.78 |
| MTT (s) | 4.47 ± 0.86 | 4.73 ± 1.24 | 3.05 ^{b,c} | 4.96 | 4.93 ± 0.23 |
| Caudate | | | | | |
| ADC (×10 ⁻³ mm ² /s) | 0.84 ± 0.05 | 0.86 | 0.67 ^{b,c} | 0.61 ^{b,c} | 1.02 ± 0.16 ^d |
| FDG SUV _{bsa} | 0.22 ± 0.01 | 0.16 ± 0.02 ^b | — | 0.09 ^{b,c} | 0.16 ± 0.03 ^b |
| CBF (ml/100 g/min) | 68.23 ± 2.95 | 85.47 ± 2.03 | 112.92 ^{d,e} | 43.10 ^{b,c} | 66.98 ± 26.61 |
| CBV (ml/100 g) | 4.55 ± 0.29 | 6.15 ± 1.54 ^d | 4.10 ^c | 3.43 ^{b,c} | 5.74 ± 2.69 |
| MTT (s) | 4.00 ± 0.152 | 4.65 ± 1.22 | 2.23 ^{b,c} | 4.79 | 6.51 ± 6.02 |
| Thalamus | | | | | |
| ADC (×10 ⁻³ mm ² /s) | 0.89 ± 0.05 | 0.90 | 0.79 | 1.18 | 0.98 ± 0.12 ^d |
| FDG SUV _{bsa} | 0.22 ± 0.02 | 0.18 ± 0.04 | — | 0.16 | 0.17 ± 0.01 |
| CBF (ml/100 g/min) | 56.20 ± 4.67 | 70.87 ± 24.41 | 43.21 | 35.29 ^b | 88.09 ± 7.71 ^d |
| CBV (ml/100 g) | 4.11 ± 0.49 | 5.90 ± 0.47 ^d | 2.61 ^c | 2.26 ^c | 5.80 ± 1.91 |
| MTT (s) | 4.40 ± 0.49 | 5.39 ± 1.52 | 3.67 | 3.83 | 3.90 ± 0.99 |
| Cortical Gray Matter | | | | | |
| ADC (×10 ⁻³ mm ² /s) | 0.88 ± 0.08 | 0.90 | 0.89 | 0.91 | 0.96 ± 0.10 ^d |
| FDG SUV _{bsa} | 0.21 ± 0.02 | 0.18 ± 0.02 ^b | — | 0.18 ^b | 0.22 ± 0.01 ^e |
| CBF (ml/100 g/min) | 61.31 ± 4.51 | 75.69 ± 25.29 | 78.09 | 63.36 | 84.06 ± 7.90 ^d |
| CBV (ml/100 g) | 4.61 ± 0.81 | 5.87 ± 0.35 ^d | 3.0 ^{b,c} | 3.47 ^{b,c} | 5.91 ± 0.89 ^d |
| MTT (s) | 5.05 ± 0.42 | 4.70 ± 1.32 | 2.82 | 3.33 | 4.32 ± 0.23 |
| White Matter | | | | | |
| ADC (×10 ⁻³ mm ² /s) | 1.05 ± 0.101 | 1.05 | 0.99 | 1.43 | 1.36 ± 0.29 ^{d,e} |
| FDG SUV _{bsa} | 0.08 ± 0.01 | 0.08 ± 0.01 | — | 0.08 | 0.07 ± 0.01 |
| CBF (ml/100 g/min) | 28.40 ± 8.08 | 30.18 ± 14.42 | 22.29 | 34.41 | 25.60 |
| CBV (ml/100 g) | 2.99 ± 0.31 | 4.07 ± 1.89 | 2.91 | 3.37 | 2.65 |
| MTT (s) | 7.18 ± 1.56 | 7.19 ± 1.12 | 8.25 | 5.89 | 6.21 |

^aAcute cytotoxic and sub-acute vasogenic columns list mean values only (two data points for each determination).^bLower than control.^cLower than non-injured GAI.^dHigher than control.^eHigher than non-injured GAI (one-way ANOVA, Tukey post-test $P < 0.05$).Abbreviations: ADC = apparent diffusion coefficient; FDG SUV_{bsa} = fluorodeoxyglucose standard uptake value corrected for body surface area; CBF = cerebral blood flow; CBV = cerebral blood volume; MTT = mean blood transit time.**Fig. 4** Vein of Galen diameter. The vein of Galen (arrows), measured in two axes on coronal T2 slices, was distended in GAI patients with atrophic (gray circles) and acute (white circles) striatal lesions. These changes in venous diameter represent estimated increases of venous blood volume of 1.5- to 3-fold during the chronic and acute phases of injury, respectively (based on the volume of a cylinder). The MRI in the far right panel is from the child described in Case I. Data were not sufficient to measure vein of Galen diameters in asymptomatic infants. Bars represent mean \pm 95% CI.

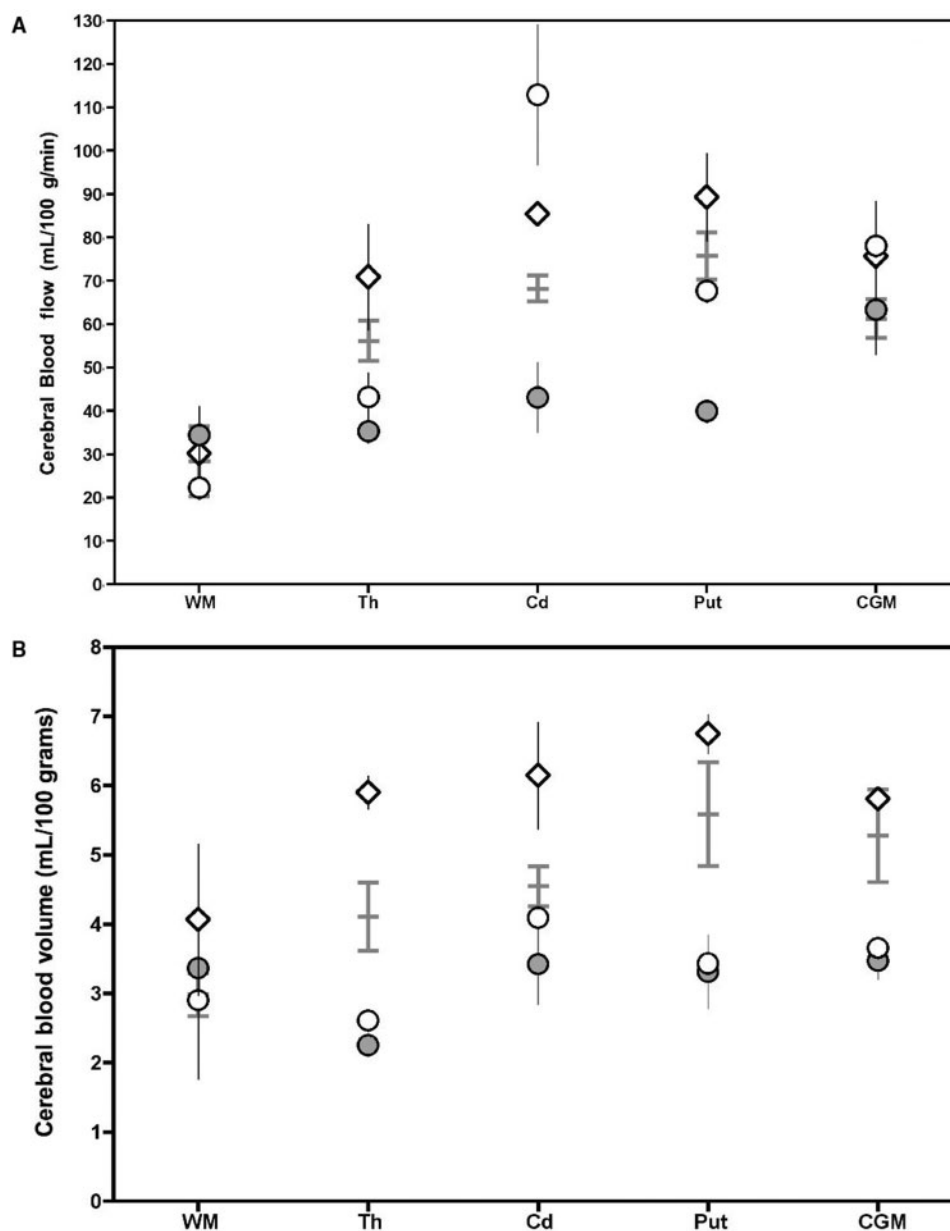


Fig. 5 Dynamic perfusion changes (mean \pm SEM). For each region of interest, control data consisted of four measurements taken from two unaffected children (ages 7 and 79 months), and are shown as gray mean \pm 2 standard deviation bars. **(A)** Cerebral blood flow (ml/100 g/min), **(B)** cerebral blood volume (ml/100 g) and **(C)** mean capillary transit time (seconds). During the acute cytotoxic phase of striatal injury in an 8-month-old child (white circles), perfusion of the caudate was high and the distribution of flow was abnormal. A follow-up PCT scan of the same patient 90 h later, during the sub-acute stage (gray circles), shows ischaemia of the striatum due to increased capillary transit time; ADC values in the caudate and putamen were low (Fig. 1D). There was a non-significant trend toward hyperperfusion in asymptomatic children (white diamonds) as a result of high CBV (Table 4). *Abbreviations:* see Fig. 1.

of the caudate and putamen (43.1 and 40.1 ml/100 g/min, respectively). An MRI at this time showed symmetric basal ganglia lesions with a heterogeneous pattern of water diffusion (Fig. 2D). The anterior striatum was swollen and had low ADC values ($0.55\text{--}0.67 \times 10^{-3} \text{ mm}^2/\text{s}$, normal $0.84 \pm 0.05 \times 10^{-3} \text{ mm}^2/\text{s}$) consistent with acute cytotoxic oedema, while the posterior-lateral putamen had high ADC values ($1.26 \times 10^{-3} \text{ mm}^2/\text{s}$), indicating old lesions (Walker *et al.*, 2004).

Opening pressure of the thecal sac was 14 cm H₂O (normal for age <20 cm H₂O). There was no evidence of encephalitis (CSF white blood cells 0, neopterin 13 nmol/l) or blood-brain barrier dysfunction (CSF IgG 1.6 mg/dl, serum IgG 513 mg/dl; CSF LDH 14 IU/l, serum LDH 224 IU/l) (Reiber, 1998). Cerebrospinal fluid glucose (59 mg/dl, CSF/serum ratio 0.6), lactate (2.1 mmol/l), amino acids (lysine 20 $\mu\text{mol/l}$, tryptophan <7 $\mu\text{mol/l}$, glutamate 1.3 $\mu\text{mol/l}$, glutamine 462 $\mu\text{mol/l}$) and

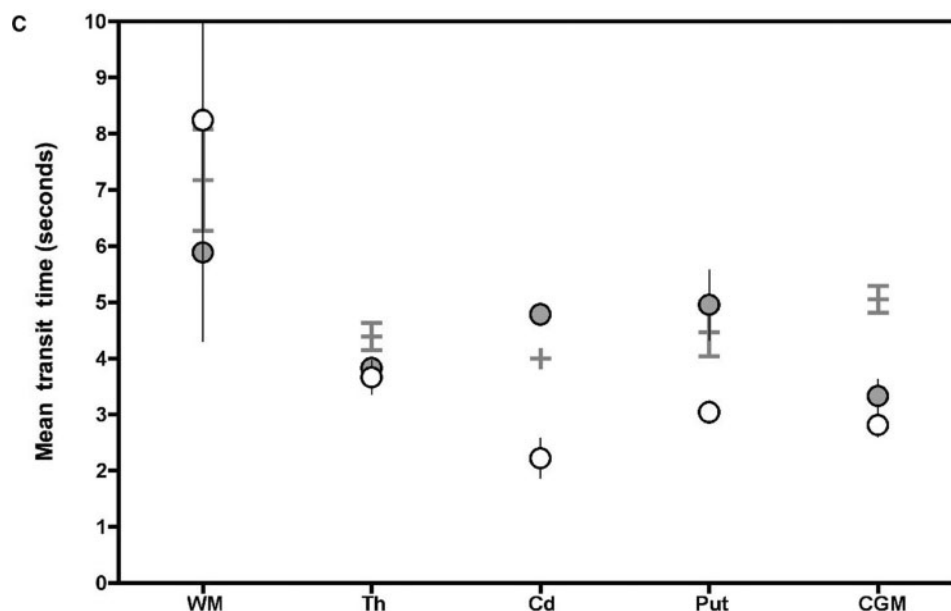


Fig. 5 Continued.

neurotransmitter metabolites were normal. Organic acid concentrations of CSF (glutarate $6.6 \mu\text{mol/l}$, 3-hydroxyglutarate $0.45 \mu\text{mol/l}$) were similar to those of plasma (glutarate $10.1 \mu\text{mol/l}$, 3-hydroxyglutarate $0.53 \mu\text{mol/l}$). CSF neuron-specific enolase, a marker for neuronal lysis, was elevated for age (21.8 ng/ml ; normal $1.52 \pm 1.01 \text{ ng/ml}$) (Rodriguez-Nunez *et al.*, 1999).

Over the course of hospitalization, opithotonus evolved into flaccidity and loss of hand use, but the child never developed generalized encephalopathy or convulsions. He made no motor progress over ensuing months and he had crippling dystonia by 1 year of age. A brain MRI 3 months after the acute event showed high water diffusion and severe atrophy of the striatum (Fig. 2C).

Case 3: striatal lesions in a newborn

An Amish boy born at term in the Midwestern United States was diagnosed with GA1 by newborn screening. During his first 2 weeks of life, he was managed at a university metabolic clinic, where he was treated with L-carnitine, a natural protein restriction of 0.9 g/kg/day , and a commercially available GA1 infant formula (Ross Metabolics, Abbott Park, IL, USA) to provide an additional 0.8 g/kg/day of lysine- and tryptophan-free L-amino acids. The family came to our clinic in Pennsylvania for an evaluation. The boy had skeletal club feet, but was otherwise healthy. Weight (3.6 kg , 50th percentile) and head circumference (38 cm , 90th percentile) were normal. Neurological exam revealed normal posture, tone, limb movements and infant reflexes. A brain MRI at 17 days of age showed posterior putaminal lesions. High regional water diffusion ($\text{ADC} = 1.6 \times 10^{-3} \text{ mm}^2/\text{s}$; Fig. 2E) indicated that these injuries were at least 10 days old

(Walker *et al.*, 2004). The child subsequently had motor delay, and by age 10 months he was fully disabled by dystonia.

Case 4: insidious motor delay and emergence of a movement disorder

An Amish girl, born to carriers of the *GCDH* 1296C>T mutation, was admitted to hospital at 14 h of age after diagnosis of GA1 by analysis of cord blood and amniotic fluid. She received dextrose and intravenous L-carnitine during an otherwise uneventful 48 h transitional period, and she was started on protein restriction (lysine intake $66 \pm 3 \text{ mg/kg/day}$), lysine-free L-amino acids (0.6 g/kg/day) and L-carnitine (65 mg/kg/day). She was not treated with an anticonvulsant, and her parents requested no immunizations be given. Growth was normal (weight 25th percentile, length 50th percentile and head circumference 50th percentile). She had mild bronchiolitis and otitis media at age 3 months but was otherwise healthy throughout infancy. Central hypotonia was noted by 4 months of age, and by age 5 months she had upper limb chorea and fisting. A brain MRI at 6 months of age showed high-diffusion lesions of the posterior-lateral putamen ($\text{ADC} = 1.2 \times 10^{-3} \text{ mm}^2/\text{s}$) as well as mildly elevated ADC values throughout the brain (Table 4).

Brain imaging results

Brain images were grouped according to three main clinical contexts: asymptomatic, acute motor regression (e.g. Cases 1 and 2) and insidious motor delay (e.g. Cases 3 and 4). For children with acute motor regression, imaging studies

were further subdivided into an early *cytotoxic* stage, a sub-acute *vasogenic* stage and a late *atrophic* stage. Quantitative imaging data for key regions of interest are summarized in Table 4.

Asymptomatic children

Only a few studies were done on asymptomatic children (Table 3). For one asymptomatic child (age 2 years), regional ADC values were normal (Table 4). PET scans of two asymptomatic infants (ages 6 and 9 months) showed reduced FDG uptake in the putamen (-29% , $P < 0.05$), caudate (-28% , $P < 0.01$), cerebellum (-26% , $P < 0.001$) and cortical gray matter (-14% , $P < 0.05$) (Fig. 3A, white diamonds). In two other asymptomatic children (ages 12 and 20 months), PCT scans showed increased blood volume and flow throughout the gray matter ($P < 0.001$; Table 4; Fig. 5, white diamonds). All five of these children remain neurologically healthy at their present ages of 3 to 5 years.

Three stages of acute motor regression

Acute cytotoxic stage

We had only one digital MRI file that was obtained during the very early stage of striatal injury and was also suitable for ADC mapping. This was designated the acute *cytotoxic* stage, 10 h after the onset of motor regression, and is shown in Fig. 2A. The MRI with ADC map depicts reduced water diffusion within the basal ganglia but no physical swelling. This signifies a regional shift of brain water from the extracellular to the intracellular space (Albers, 1998), and is a sign of potentially reversible neuronal energy failure (Fiehler *et al.*, 2002; Sakoh *et al.*, 2003). A PCT scan of an Amish boy (Case 2) done 10 h after the onset of regression showed decreased blood volume and fast transit throughout the gray matter. These changes did not affect regional perfusion uniformly (Fig. 5, white circles): flows to the putamen and thalamus were slightly reduced, cortical perfusion was normal, and perfusion of the caudate was augmented by 65% ($P < 0.01$).

Sub-acute vasogenic stage

Ninety hours later, a PCT scan of the same child (Case 2; Fig. 5, gray circles) showed prolongation of transit times in the caudate ($+62\%$) and putamen ($+40\%$), rendering these structures ischemic relative to the cortex and thalamus (Rohl *et al.*, 2001). ADC values were low within the hypoperfused basal ganglia and normal within the cortex and thalamus (Fig. 2C). Another Amish child (Case 1) was also imaged at the sub-acute stage, 5 days after the onset of motor regression (Fig. 2B). Her basal ganglia were swollen and had diffusion values that were 'pseudo-normal', reflecting a composite of *cytotoxic* (low intracellular diffusion) and *vasogenic*

(high extracellular diffusion) oedema (Lansberg *et al.*, 2001; Ironside and Pickard, 2002). A PET scan done within the same time period showed markedly reduced striatal FDG uptake (Fig. 3A, white circles).

Chronic atrophic stage

All nine disabled children from the 1995–2005 cohort had at least one MRI done several months after the onset of clinical signs. We designated this the *atrophic* stage, depicted in Fig. 2C. At this late stage, lesions were static and all looked similar. The striatum was shrunken and had high water diffusion, reflecting neuronal loss and gliosis (Funk *et al.*, 2005). In contrast, the pallidum was often normal, suggesting recovery from the cytotoxic stage. Although the striatum was the only region that consistently showed signs of atrophy, ADC values were mildly elevated throughout the brain (Table 4). Four of nine children had other imaging studies during the chronic stage: two children had PET scans (at ages 10 and 12 years) that showed reduced glucose uptake in the putamen (-60% , $P < 0.001$) (Fig. 3B), and two children had PCT scans (at ages 6 and 20 months) that showed elevated thalamic and cortical perfusion ($P < 0.05$) due to regional hyperaemia (Table 4).

Insidious motor delay and the timing of brain injury

The onset of brain injury could not be determined in six of nine cases that occurred after 1994. All six of these children had a similar clinical course: hypotonia of the trunk was recognized between 2 and 3 months of age, independent sitting was delayed, and a movement disorder emerged gradually between 4 and 6 months of age. Although these children had similar MRI findings during the late stage (Fig. 2C), we nonetheless recognized four distinctive clinical patterns among them:

- (1) Two children had MRI studies at approximately 2 weeks of age. Although they appeared healthy at the time, ADC maps revealed high-diffusion lesions of the putamen (Case 3; Fig. 2E). Based on the diffusion values, these lesions were at minimum 10 days old (Lansberg *et al.*, 2001; Walker *et al.*, 2004; Barkovich *et al.*, 2006) and might have occurred before birth. Both children subsequently had motor delay and developed dystonia by 6 months of age.
- (2) Two sisters were healthy throughout the perinatal period and early infancy, but by 6 months of age were hypotonic, not sitting and had mild chorea. In both cases, MRI studies revealed atrophic striatal lesions (Case 4; see e.g. Fig. 2C).
- (3) One child was thought to have sudden onset of dystonia at 8 months of age during an infectious illness, but an ADC map revealed chronic atrophic

Table 5 Contingency tables for treatment intervention (row) versus neurological outcome (column) in 48 Amish GAI patients

| Intervention | N | Percent injured | Odds ratio for disability (95% CI) ^a | P-value ^a |
|---|----|-----------------|---|----------------------|
| Diagnosis by newborn screening | 31 | 36 | 0.04 (0.01–0.34) | <0.001 |
| L-carnitine therapy | 25 | 36 | 0.56 (0.09–3.40) | 0.653 |
| Lysine-free L-amino acid supplementation ^b | 10 | 30 | 0.62 (0.13–3.06) | 0.703 |
| Hospitalization for neonatal transition | 11 | 38 | 0.79 (0.17–3.59) | 1.000 |
| Prophylactic anticonvulsant, 0–6 months | 14 | 38 | 0.79 (0.18–4.20) | 1.000 |
| Vitamin cofactor supplementation ^c | 10 | 40 | 1.08 (0.23–5.06) | 1.000 |
| Immunization | 19 | 46 | 2.70 (0.55–13.20) | 0.274 |

^aTwo-sided Fisher's exact test.^bComposition, in mg/g protein: tryptophan 20, alanine 100, arginine 50, carnitine 100, glutamine 150, glycine 20, histidine 20, isoleucine 50, leucine 100, methionine 20, phenylalanine 50, serine 20, taurine 10, threonine 50, tyrosine 50 and valine 50.^cVitamin intakes: creatine, 50 mg/kg/day, and 10 mg/kg/day each of alpha-lipoate, coenzyme Q10, pantothenate, thiamine and riboflavin.

high-diffusion lesions and no acute changes. Rather, there was 'sudden' clinical recognition of latent brain lesions.

- (4) One child presented with sudden motor regression superimposed on chronic motor delay (Case 2). There was evidence of two discrete injuries, separated in time. When imaged during a cerebral crisis at 8 months of age, he had acute caudate lesions (restricted diffusion and oedema) anterior to chronic lesions (high diffusion and atrophy) of the posterior–lateral putamen (Fig. 2D).

Venous blood volume in injured children

The vein of Galen was distended during both the sub-acute (+70%, $P < 0.001$) and chronic (+30%, $P < 0.001$) stages of brain injury (Fig. 4). We considered this a marker for increased blood volume within the deep cerebral venous system. Modeling the vein of Galen as a cylinder, the observed changes of diameter would signify 1.5- to 3-fold increases of volume. We did not have enough digital MRI data to determine vein of Galen diameters in asymptomatic children with GAI (Table 3).

The effects of treatment on neurological outcome

After 1994, the incidence of brain injury did not vary significantly by birth year or treatment strategy (Table 1), and clinical and biochemical parameters were similar between brain-injured and asymptomatic groups (Table 2). Diagnosis of GAI during the newborn period (31 of 48 Amish patients), followed by a prescribed diet and intravenous fluid and dextrose therapy during illnesses, reduced the risk of brain injury ($P < 0.001$) (Tables 1 and 5). Brain lesions tended to be less severe in patients diagnosed as newborns (OR for severe injury = 0.18, 95%CI = 0.03–1.23, $P = 0.14$). Only 12% of brain-injured patients born before 1990 achieved any level of independence, whereas 44% of those injured after 1995 could walk, speak, eat and use their hands.

Paired contingency analyses of other treatment variables showed only insignificant trends in favour of L-carnitine and lysine-free L-amino acid therapy (Table 5). Neither prophylactic anticonvulsants nor vitamin cofactors were protective, and we subsequently stopped prescribing them. We found a trend toward higher risk of brain injury in immunized patients (OR = 2.7), but this result was not significant ($P = 0.27$).

Children with brain injury were 20 times more likely to die young than asymptomatic children with GAI (95%CI = 1.1–367.0, $P = 0.006$). There were nine deaths among a total of 28 brain-injured Amish patients followed since 1989. Three children died from complications of dystonia (pulmonary aspiration and esophageal perforation), whereas six disabled children died suddenly and unexpectedly from undetermined causes.

Discussion

Acute striatal necrosis from GAI is a relatively rare event in children with an uncommon disorder. Consequently, there are precious few imaging studies of the type presented here (Table 3). We recognize this as a limitation of the present work, and thus our observations should be interpreted with caution. Nevertheless, we were able to use a series of imaging studies to correlate clinical events (see e.g. Cases 1–4) with physiological data about cerebral water diffusion, glucose uptake and blood flow. Our results show clearly that 'metabolic stroke' in living subjects is a complex and dynamic process (Clarke and Sokoloff, 1999) that consists of both metabolic and hemodynamic components. We propose three stages of this process, and identify physiological disturbances that may occur *in vivo* at each stage.

Cerebral metabolism in GAI

In individuals with GAI, glutaryl-CoA and its derivatives, glutarate and 3-hydroxyglutarate, probably begin to accumulate in brain and other tissues during fetal life.

These compounds are not readily transported out of brain cells (Hassel *et al.*, 2002; Strauss, 2005; Sauer *et al.*, 2006) and during infancy can reach levels as high as 2000 $\mu\text{mol/kg}$ of brain tissue (Funk *et al.*, 2005), orders of magnitude above concentrations in plasma or cerebrospinal fluid (Table 2; Case 2).

There has been speculation based on *in vitro* data that high cerebral concentrations of glutarates or their glutaryl-CoA precursor inhibit oxidative phosphorylation in the brain (Sauer *et al.*, 2005). Our PET findings support this idea (Table 4, Fig. 3A), and suggest that brain injury from GAI may be similar in principle to 3-nitropropionic acid poisoning (Brouillet *et al.*, 1995; Brownell *et al.*, 2004). According to this paradigm, chronic exposure to a histotoxin (i.e. glutaryl-CoA or glutarate) can reduce energy production in neurons and predispose them to injury (Calabresi *et al.*, 2000). We interpreted reduced FDG uptake as evidence of this predisposition (Fig. 3A, white diamonds).

In vitro, striatal neurons can suddenly depolarize and die when energy production falls below a critical threshold, estimated to be 50–60% of their normal metabolic rate (Riepe *et al.*, 1995; Brouillet *et al.*, 1998). Striatal metabolism was probably at or below this viability limit during the earliest stage of brain injury (Fig. 2A), as shown by a 20–30% decrease of regional water diffusion 10 h after the onset of motor regression. Extrapolating from animal studies, this signifies a 50% decrease of regional metabolic rate (Sakoh *et al.*, 2000, 2003). Alterations of cerebral blood flow did not account for this change (Fig. 5A, white circles) (Bristow *et al.*, 2005; Arakawa *et al.*, 2006), suggesting that intrinsic energy failure of neurons was the first step in the degenerative process. The morphology of early diffusion changes was further evidence of primary energy failure (Fig. 2A): the lesions were symmetric and sharply demarcated by histological, rather than vascular, boundaries.

Cerebral blood flow in GAI

At the beginning of cerebral crisis, 10 h after the onset of clinical signs (Case 2; Fig. 5, white circles), blood volume and transit time were reduced throughout the gray matter. A PCT study of the same child 90 h later showed a 40–50% decrease of striatal perfusion due almost exclusively to prolongation of capillary transit time (Fig. 5C, gray circles). During the sub-acute stage, fluid from the circulation entered the basal ganglia. This was seen as focal swelling (Ayata and Ropper, 2002) and ‘normalization’ of regional ADC values, reflecting accumulation of extracellular fluid within damaged tissues (Fig. 2B). Such changes indicate a disturbance of the blood–brain barrier (Ito *et al.*, 2003), and can exacerbate tissue injury (Hamilton and Gould, 1987; Hudetz, 1997a; Pranevicius and Pranevicius, 2002; Ito *et al.*, 2003).

Oligemia persisted in all gray matter regions throughout a cerebral crisis, but fast blood transit kept the cortex well perfused (Table 4; Fig. 5, gray circles) (Arakawa *et al.*, 2006). This finding raises the interesting possibility that selective vulnerability of the striatum is related to disparate hemodynamic responses in various brain regions; i.e. when cerebral blood volume is globally reduced (Fig. 5), areas such as the cortex that can recruit more flow may have a survival advantage. This is consistent with a hypothesis by Auer and Sutherland (2002) that for neurons to die from a histotoxin they must also suffer a simultaneous disturbance of blood flow.

Interactions between metabolism and blood flow

Cerebral blood volume and flow were elevated in two asymptomatic children with GAI (Fig. 5, white diamonds). Hyperaemia also occurs in hypoxaemia (Shockley and LaManna, 1988; Hudetz, 1997b) and 3-nitropropionic acid poisoning (Chyi and Chang, 1999). Considering the close interdependence of cerebral metabolism and perfusion (Clarke and Sokoloff, 1999; Sakoh *et al.*, 2000), augmentation of blood volume and flow in all these conditions may represent appropriate compensations by the cerebral circulation to reduced substrate oxidation.

A reciprocal relationship between cerebral glucose oxidation and blood flow would clarify how brain injuries occur in GAI. Viewed in this context, cerebral accumulation of a histotoxin may predispose a child to striatal lesions, but is not a committal step in the process. Additional circumstances that either aggravate metabolic toxicity or decrease regional perfusion may be necessary to lower striatal energy production to the threshold for membrane failure (Riepe *et al.*, 1995). This may also explain why infusion of 10% dextrose during illnesses is neuroprotective (Table 5): this intervention simultaneously increases the concentration of glucose in plasma and its rate of delivery to the brain.

Indeed, we believe that the major therapeutic advantage of newborn screening for GAI is the ability to promptly intervene with intravenous therapy during illnesses. Between 1990 and 2005, we managed 119 hospitalizations of GAI patients for unstable neonatal transitions ($n=12$), intracranial bleeding ($n=2$), seizures ($n=4$), traumas or surgeries ($n=21$) and gastrointestinal or respiratory infections ($n=80$), many of them severe. Throughout this time period, no patient ever regressed while in the hospital on intravenous fluid and dextrose therapy. In contrast, brain injury was predictable when emergency therapy was delayed (Case 1), and inpatient management was not effective for children who presented to the hospital with clinical and radiological signs of neurological damage (Cases 1 and 2).

Changes of the deep cerebral venous system

Engorgement of the deep venous system was observed during both the sub-acute and chronic stages of brain injury (Case 1; Fig. 4). Unfortunately, we did not have an adequate number of MRI studies to measure vein of Galen diameters in asymptomatic children. During the chronic and sub-acute stages, venous congestion may occur for different reasons. Chronically, large cerebral veins might simply reflect global hyperaemia (i.e. high capillary blood volume and flow) (Fig. 5, white diamonds), whereas acutely, venous blood volume may increase as a result of abnormal autoregulation and arteriovenous shunting (i.e. low capillary blood volume and flow) (Hudetz, 1997a; Edelman and Hoffman, 1999).

Further studies are necessary to better understand the relevance of these changes in the deep venous system. However, it is worth noting that congestion of deep cerebral veins could explain several peculiar features of GA1 (Ursino *et al.*, 1998; Morris *et al.*, 1999; Gass *et al.*, 2001; Ironside and Pickard, 2002; Strauss *et al.*, 2003; Strauss, 2005) including increased brain weight (Strauss, 2005), hydrocephalus (Martinez-Lage, 1996), white matter vacuolization (Chow *et al.*, 1988) and the propensity for subdural and retinal hemorrhages (Strauss *et al.*, 2003). Increased venous volume and pressure could also account for capillary dilation, interstitial vacuolization and haemorrhages seen in lysine-fed *Gcdh*^{−/−} mice (Zinnanti *et al.*, 2006).

How does treatment of GA1 change clinical outcome?

Our observations blur the distinction between acute and insidious presentations of motor disability in children with GA1. We suspect these two clinical patterns differ only in timing: insidious motor delay may simply reflect acute striatal degeneration that pre-dates clinical awareness. We provide direct evidence of this latency phenomenon in Amish patients (see e.g. Case 3; Fig. 2E), which has two important implications for the interpretation of treatment and outcome data in outbred populations. First, in many cases it is impossible to determine when treatment (e.g. diet, L-carnitine) was introduced relative to brain injury. Second, a sub-group of GA1 patients may develop striatal degeneration before any opportunity for clinical intervention (Case 3). These facts confound efforts to interpret data from cross-sectional surveys (Kolker *et al.*, 2006). Indeed, in our experience with Amish GA1 patients, traditional dietary and biochemical indices of ‘metabolic control’ (Table 2) provide no information about neurological risk. We conclude that more *in vivo* data, building upon the observations presented here, are needed to improve medical care for children with GA1.

Supplementary material

Supplementary material are available at *Brain* online.

Acknowledgements

The authors thank Drs Julie Mack and Scott Winner for their help interpreting imaging studies. The workstation and software used for MRI analyses were graciously donated to the non-profit Clinic for Special Children (EIN23-2555373) by the A.J. Stamps Foundation. Drs Silvia Tortorelli, Dietrich Matern, and Piero Rinaldo donated time and expertise for biochemical analyses. The staff and administration of the PET Diagnostic Imaging Center graciously donated machine time and expertise for obtaining PET studies. The authors thank Christine Weir and her colleagues at the MRI group, as well as the paediatric nursing staff at Lancaster General Hospital. Dr Richard Kelley provided guidance and helpful editorial suggestions during the preparation of the manuscript. Finally, the authors thank children with GA1 and their patients; they continue to be our most important teachers. Funding to pay the Open Access publication charges for this article was provided by the Clinic for Special Children, in part using charitable donations from the Amish and Mennonite communities.

References

- Albers GW. Diffusion-weighted MRI for evaluation of acute stroke. *Neurology* 1998; 51: S47–9.
- Arakawa S, Wright PM, Koga M, Phan TG, Reutens DC, Lim I, et al. Ischemic thresholds for gray and white matter: a diffusion and perfusion magnetic resonance study. *Stroke* 2006; 37: 1211–6.
- Auer RN, Sutherland GR. Hypoxia and related conditions. In: Graham DI, Lantos PL, editors. *Greenfield's neuropathology*. (Vol. 1): London: Arnold; 2002. p. 233–80.
- Ayata C, Ropper AH. Ischaemic brain oedema. *J Clin Neurosci* 2002; 9: 113–24.
- Barkovich AJ, Miller SP, Barth A, Newton N, Hamrick SE, Mukherjee P, et al. MR imaging, MR spectroscopy, and diffusion tensor imaging of sequential studies in neonates with encephalopathy. *AJNR Am J Neuroradiol* 2006; 27: 533–47.
- Bristow MS, Simon JE, Brown RA, Eliasziw M, Hill MD, Coutts SB, et al. MR perfusion and diffusion in acute ischemic stroke: human gray and white matter have different thresholds for infarction. *J Cereb Blood Flow Metab* 2005; 25: 1280–7.
- Brouillet E, Guyot MC, Mittoux V, Altairac S, Conde F, Palfi S, et al. Partial inhibition of brain succinate dehydrogenase by 3-nitropropionic acid is sufficient to initiate striatal degeneration in rat. *J Neurochem* 1998; 70: 794–805.
- Brouillet E, Hantraye P, Ferrante RJ, Dolan R, Leroy-Willig A, Kowall NW, et al. Chronic mitochondrial energy impairment produces selective striatal degeneration and abnormal choreiform movements in primates. *Proc Natl Acad Sci USA* 1995; 92: 7105–9.
- Brownell AL, Chen YI, Yu M, Wang X, Dedeoglu A, Cicchetti F, et al. 3-Nitropropionic acid-induced neurotoxicity—assessed by ultra high resolution positron emission tomography with comparison to magnetic resonance spectroscopy. *J Neurochem* 2004; 89: 1206–14.
- Calabresi P, Centonze D, Bernardi G. Cellular factors controlling neuronal vulnerability in the brain: a lesson from the striatum. *Neurology* 2000; 55: 1249–55.
- Chow CW, Haan EA, Goodman SI, Anderson RM, Evans WA, Kleinschmidt-DeMasters BK, et al. Neuropathology in glutaric acidemia type 1. *Acta Neuropathol (Berl)* 1988; 76: 590–4.

- Chyi T, Chang C. Temporal evolution of 3-nitropropionic acid-induced neurodegeneration in the rat brain by T2-weighted, diffusion-weighted, and perfusion magnetic resonance imaging. *Neuroscience* 1999; 92: 1035–41.
- Clarke DD, Sokoloff L. Circulation and energy metabolism of the brain. In: Siegel GJ, Agranoff BW, Albers RW, Fisher SK, Uhler MD, editors. *Basic Neurochemistry: Molecular, Cellular, and Medical Aspects*. Philadelphia: Lippincott-Raven; 1999. p. 637–70.
- Edelman G, Hoffman WE. Cerebral venous and tissue gases and arteriovenous shunting in the dog. *Anesth Analg* 1999; 89: 679–83.
- Erecinska M, Cherian S, Silver IA. Energy metabolism in mammalian brain during development. *Prog Neurobiol* 2004; 73: 397–445.
- Fiehler J, Foth M, Kucinski T, Knab R, von Bezold M, Weiller C, et al. Severe ADC decreases do not predict irreversible tissue damage in humans. *Stroke* 2002; 33: 79–86.
- Funk CB, Prasad AN, Frosk P, Sauer S, Kolker S, Greenberg CR, et al. Neuropathological, biochemical and molecular findings in a glutaric acidemia type 1 cohort. *Brain* 2005; 128: 711–22.
- Gass A, Niendorf T, Hirsch JG. Acute and chronic changes of the apparent diffusion coefficient in neurological disorders—biophysical mechanisms and possible underlying histopathology. *J Neurol Sci* 2001; 186 (Suppl 1): S15–23.
- Haas RH, Marsden DL, Capistrano-Estrada S, Hamilton R, Grafe MR, Wong W, et al. Acute basal ganglia infarction in propionic acidemia. *J Child Neurol* 1995; 10: 18–22.
- Hamilton BF, Gould DH. Nature and distribution of brain lesions in rats intoxicated with 3-nitropropionic acid: a type of hypoxic (energy deficient) brain damage. *Acta Neuropathol (Berl)* 1987; 72: 286–97.
- Hassel B, Brathe A, Petersen D. Cerebral dicarboxylate transport and metabolism studied with isotopically labelled fumarate, malate and malonate. *J Neurochem* 2002; 82: 410–9.
- Hoffmann GF, Gibson KM, Trefz FK, Nyhan WL, Bremer HJ, Rating D. Neurological manifestations of organic acid disorders. *Eur J Pediatr* 1994; 153: S94–100.
- Hudetz AG. Blood flow in the cerebral capillary network: a review emphasizing observations with intravital microscopy. *Microcirculation* 1997a; 4: 233–52.
- Hudetz AG. Regulation of oxygen supply in the cerebral circulation. *Adv Exp Med Biol* 1997b; 428: 513–20.
- Ironside JW, Pickard JD. Raised intracranial pressure, oedema, and hydrocephalus. In: Graham DI, Lantos PL, editors. *Greenfield's Neuropathology*. (Vol. 1). London: Arnold; 2002. p. 193–232.
- Ito U, Kuroiwa T, Hanyu S, Hakamata Y, Kawakami E, Nakano I, et al. Temporal profile of experimental ischemic edema after threshold amount of insult to induce infarction—ultrastructure, gravimetry and Evans' blue extravasation. *Acta Neurochir Suppl* 2003; 86: 131–5.
- Kolker S, Garbade SF, Greenberg CR, Leonard JV, Saudubray JM, Ribes A, et al. Natural history, outcome, and treatment efficacy in children and adults with glutaryl-CoA dehydrogenase deficiency. *Pediatr Res* 2006; 59: 840–7.
- Kolker S, Hoffmann GF, Schor DS, Feyh P, Wagner L, Jeffrey I, et al. Glutaryl-CoA dehydrogenase deficiency: region-specific analysis of organic acids and acylcarnitines in post mortem brain predicts vulnerability of the putamen. *Neuropediatrics* 2003; 34: 253–60.
- Lansberg MG, Thijs VN, O'Brien MW, Ali JO, de Crespigny AJ, Tong DC, et al. Evolution of apparent diffusion coefficient, diffusion-weighted, and T2-weighted signal intensity of acute stroke. *AJNR Am J Neuroradiol* 2001; 22: 637–44.
- Martinez-Lage JF. Neurosurgical treatment for hydrocephalus, subdural hematomas, and arachnoid cysts in glutaric aciduria type 1. *Neuropediatrics* 1996; 27: 335–6.
- Morris AA, Hoffmann GF, Naughten ER, Monavari AA, Collins JE, Leonard JV. Glutaric aciduria and suspected child abuse. *Arch Dis Child* 1999; 80: 404–5.
- Morton DH, Bennett MJ, Seargeant LE, Nichter CA, Kelley RI. Glutaric aciduria type I: a common cause of episodic encephalopathy and spastic paralysis in the Amish of Lancaster County, Pennsylvania. *Am J Med Genet* 1991; 41: 89–95.
- Morton DH, Morton CS, Strauss KA, Robinson DL, Puffenberger EG, Hendrickson C, et al. Pediatric medicine and the genetic disorders of the Amish and Mennonite people of Pennsylvania. *Am J Med Genet C Semin Med Genet* 2003; 121: 5–17.
- Nagesh V, Welch KM, Windham JP, Patel S, Levine SR, Hearshen D, et al. Time course of ADCw changes in ischemic stroke: beyond the human eye! *Stroke* 1998; 29: 1778–82.
- Nehlig A. Cerebral energy metabolism, glucose transport and blood flow: changes with maturation and adaptation to hypoglycaemia. *Diabetes Metab* 1997; 23: 18–29.
- Pranevicius M, Pranevicius O. Cerebral venous steal: blood flow diversion with increased tissue pressure. *Neurosurgery* 2002; 51: 1267–73; discussion 1273–4.
- Puffenberger EG. Genetic heritage of the Old Order Mennonites of Southeastern Pennsylvania. *Am J Med Genet Part C (Semin Med Genet)* 2003; 121C: 18–31.
- Reiber H. Cerebrospinal fluid—physiology, analysis and interpretation of protein patterns for diagnosis of neurological diseases. *Mult Scler* 1998; 4: 99–107.
- Riepe MW, Hori N, Ludolph AC, Carpenter DO. Failure of neuronal ion exchange, not potentiated excitation, causes excitotoxicity after inhibition of oxidative phosphorylation. *Neuroscience* 1995; 64: 91–7.
- Rodriguez-Nunez A, Cid E, Eiris J, Rodriguez-Garcia J, Camina F, Rodriguez-Segade S, et al. Neuron-specific enolase levels in the cerebrospinal fluid of neurologically healthy children. *Brain Dev* 1999; 21: 16–9.
- Rohl L, Ostergaard L, Simonsen CZ, Vestergaard-Poulsen P, Andersen G, Sakoh M, et al. Viability thresholds of ischemic penumbra of hyperacute stroke defined by perfusion-weighted MRI and apparent diffusion coefficient. *Stroke* 2001; 32: 1140–6.
- Sakoh M, Ohnishi T, Ostergaard L, Gjedde A. Prediction of tissue survival after stroke based on changes in the apparent diffusion of water (cytotoxic edema). *Acta Neurochir Suppl* 2003; 86: 137–40.
- Sakoh M, Ostergaard L, Rohl L, Smith DF, Simonsen CZ, Sorensen JC, et al. Relationship between residual cerebral blood flow and oxygen metabolism as predictive of ischemic tissue viability: sequential multi-tracer positron emission tomography scanning of middle cerebral artery occlusion during the critical first 6 hours after stroke in pigs. *J Neurosurg* 2000; 93: 647–57.
- Sauer SW, Okun JG, Fricker G, Mahringer A, Muller I, Crnic LR, et al. Intracerebral accumulation of glutaric and 3-hydroxyglutaric acids secondary to limited flux across the blood-brain barrier constitute a biochemical risk factor for neurodegeneration in glutaryl-CoA dehydrogenase deficiency. *J Neurochem* 2006.
- Sauer SW, Okun JG, Schwab MA, Crnic LR, Hoffmann GF, Goodman SI, et al. Bioenergetics in glutaryl-coenzyme A dehydrogenase deficiency: a role for glutaryl-coenzyme A. *J Biol Chem* 2005; 280: 21830–6.
- Schmithorst VJ, Dardzinski BJ, Holland SK. Simultaneous correction of ghost and geometric distortion artifacts in EPI using a multiecho reference scan. *IEEE Trans Med Imaging* 2001; 20: 535–9.
- Shockley RP, LaManna JC. Determination of rat cerebral cortical blood volume changes by capillary mean transit time analysis during hypoxia, hypercapnia and hyperventilation. *Brain Res* 1988; 454: 170–8.
- Strauss KA. Glutaric aciduria type 1: a clinician's view of progress. *Brain* 2005; 128: 697–9.
- Strauss KA, Puffenberger EG, Robinson DL, Morton DH. Type I glutaric aciduria, part 1: natural history of 77 patients. *Am J Med Genet C Semin Med Genet* 2003; 121: 38–52.
- Sugawara Y, Zasadny KR, Neuhoff AW, Wahl RL. Reevaluation of the standardized uptake value for FDG: variations with body weight and methods for correction. *Radiology* 1999; 213: 521–5.

- Ursino M, Giulioni M, Lodi CA. Relationships among cerebral perfusion pressure, autoregulation, and transcranial Doppler waveform: a modeling study. *J Neurosurg* 1998; 89: 255–66.
- Walker PM, Ben Salem D, Lalande A, Giroud M, Brunotte F. Time course of NAA T2 and ADC(w) in ischaemic stroke patients: 1H MRS imaging and diffusion-weighted MRI. *J Neurol Sci* 2004; 220: 23–8.
- Wang GJ, Volkow ND, Overall J, Hitzemann RJ, Pappas N, Pascani K, et al. Reproducibility of regional brain metabolic responses to lorazepam. *J Nucl Med* 1996; 37: 1609–13.
- Wintermark M, Lepori D, Cotting J, Roulet E, van Melle G, Meuli R, et al. Brain perfusion in children: evolution with age assessed by quantitative perfusion computed tomography. *Pediatrics* 2004; 113: 1642–52.
- Wintermark M, Thiran JP, Maeder P, Schnyder P, Meuli R. Simultaneous measurement of regional cerebral blood flow by perfusion CT and stable xenon CT: a validation study. *AJNR Am J Neuroradiol* 2001; 22: 905–14.
- Yeung HW, Sanches A, Squire OD, Macapinlac HA, Larson SM, Erdi YE. Standardized uptake value in pediatric patients: an investigation to determine the optimum measurement parameter. *Eur J Nucl Med Mol Imaging* 2002; 29: 61–6.
- Zinnanti WJ, Lazovic J, Wolpert EB, Antonetti DA, Smith MB, Connor JR, et al. A diet-induced mouse model for glutaric aciduria type I. *Brain* 2006.